Applied Catalysis A: General 409–410 (2011) 140–147

Contents lists available at SciVerse ScienceDirect

Applied Catalysis A: General

journal homepage: www.elsevier.com/locate/apcata

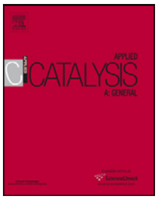

Design of improved hydrocracking catalysts by increasing the proximity between acid and metallic sites

J. Francis[a], E. Guillon[a,*], N. Bats[a], C. Pichon[a], A. Corma[b], L.J. Simon[a]

[a] IFP Energies nouvelles, Rond-point de l'échangeur de Solaize, BP 3, 69360 Solaize, France
[b] Instituto de Tecnología Química CSIC-UPV, Universidad Politécnica de Valencia, Av. De los Naranjos s/n, 46022 Valencia, Spain

ARTICLE INFO

Article history:
Received 3 August 2011
Received in revised form
28 September 2011
Accepted 29 September 2011
Available online 6 October 2011

Keywords:
Hydrocracking
Squalane
Zeolite
Nickel
Metal sulfide
Proximity

ABSTRACT

A new approach was undertaken to increase the bifunctionality of USY zeolite based catalyst. Nickel metallic phase was first impregnated onto USY zeolite and composite catalysts NiMo/[γ-Al_2O_3 + (Ni)/USY] were prepared from these zeolites. Catalytic properties in toluene hydrogenation and squalane (2,6,10,15,19,23-hexamethyltetracosane) hydrocracking (HCK) were investigated.

Enhanced conversion and middle distillate (MD) selectivity was obtained for catalysts on which nickel has been impregnated on the zeolite powder. These enhancements are ascribed to an increased proximity between the hydrogenation/dehydrogenation (H/DH) function and the acid sites resulting in a more efficient synergy between these two functions.

1. Introduction

The European demand in kerosene and gas oil keeps increasing with the development of air traffic and diesel engine vehicle fleet, and improvements of processes dedicated to Middle Distillate (MD) production are of key interest. Among these, the hydrocracking (HCK) process is probably the most adequate to produce high yields of good quality MDs. Hydrocrackers are very flexible units allowing to process a wide range of feedstocks and to obtain a wide range of products [1,2]. In particular, production of high quality MD can be achieved in such units working at high hydrogen pressure and allowing the formation of highly valuable saturated products for jet or diesel fuel pools [3]. Quality of hydrocracker MD is better than FCC MD, with a lower sulfur content and an improved cetane number [4,5] in the former.

HCK catalysts are commonly bifunctional catalytic systems constituted by a hydrogenation/dehydrogenation (H/DH) and an acidic cracking components [6–8]. The H/DH component consists of noble metals, which are highly active but have a low resistance to sulfur poisoning, or by an association of a sulfided phase of a group VI element (Ni or Co) and a group VIII element (Mo or W) of the periodic table. Usually, the latter ones are preferred because of their sulfur and nitrogen resistance. A Ni–Mo sulfide phase is often chosen, due to its higher hydrogenation activity, on alumina supports [3,9]. Alumina favors a better dispersion of the H/DH function and allows better mechanical properties of catalyst extrudates [2,10,11].

The acidic function can be brought by amorphous silica–alumina or zeolites, and more specifically ultrastable Y (USY) zeolites. Zeolites are by far the most active for cracking due to their higher acidity and are now commonly used. One of the major drawbacks of zeolites for HCK is the size of the micropores, which leads to diffusion limitations resulting in excessive coking and secondary cracking of primary products [12,13]. Recent different approaches are described in the literature in order to decrease these limitations and, therefore, to improve zeolite activity and MD yields in HCK. Among those we can highlight: (i) the formation of mesopores using various techniques (dealumination, desilication) [9,14,15]; (ii) the synthesis of smaller zeolitic crystal size [16–20] to decrease diffusion barriers; (iii) the modification of USY by $Ti(SO_4)_2$ [21] or by $FeSO_4$ or $Fe(NO_3)_3$ [22–24] to increase the porosity and provide some H/DH sites into the zeolite. Another strategy can be to tune the bifunctionality of the catalyst by modifying the nature, the content and the location of the metallic phase in order to optimize the MD formation.

A generally accepted HCK reaction scheme includes five chemical steps: (i) dehydrogenation of a feed molecule on a metallic site; (ii) migration of the resultant olefin to an acid site; (iii) isomerization and/or cracking of this olefin on acid site(s); (iv) migration of the products to a metallic site; (v) hydrogenation of the reaction products [6,25,26]. One of the key parameter for the design of a

---

* Corresponding author. Tel.: +33 437702875; fax: +33 437702066.
E-mail address: emmanuelle.guillon@ifpen.fr (E. Guillon).

0926-860X/$ – see front matter © 2011 Elsevier B.V. All rights reserved.
doi:10.1016/j.apcata.2011.09.040

successful HCK catalyst is the balance between the H/DH and acidic active functions [25,27]. On an ideal bifunctional catalyst the H/DH reactions are at quasi equilibrium and the limiting step occurs on the acidic function [25]. The steady-state concentration of olefins in the vicinity of the acid sites is sufficient to quickly desorb compounds that are adsorbed on these acid sites. Then, the turnover frequency of these catalysts is high and consecutive cracking reactions and coke formation are limited, which contributes to increase activity, stability and selectivity for MD. Typically, an improvement of the balance will result in better activity and MD formation in the case of VGO HCK [18,28]. The balance between the two active functions is determined by the number and the strength of each type of sites. Guisnet et al. have shown that an ideal behavior in hydroisomerization of model molecules on a Pt/USY catalyst, can be achieved by increasing the number of accessible Pt sites [27,29–31]. Lugstein et al. have shown that a Pt/ZSM-5 catalyst has by far a better H/DH and acid sites balance than a Ni/ZSM-5 catalyst [32]. The authors explain that the intrinsic hydrogenation strength of Pt is much higher than the Ni one. The proximity between the two different sites is also thought to be important [33]. For instance, Galperin et al. have obtained better activity and selectivity for the hydroisomerization of n-decane with a Pt/(Al_2O_3 + MAPSO-31) catalyst (impregnated extrudates) than with a Pt/Al_2O_3 + MAPSO-31 (mechanical mixture) due to the enhanced proximity between the hydrogenating Pt sites and acid sites of the MAPSO-31 material [34]. Cornet et al. have also showed that impregnation of a NiMo phase on zeolite crystals, before physical mixing of the zeolite with NiMo/Al_2O_3, results in an improvement of conversion and selectivity towards isomerized products in n-decane hydroisomerization [35].

From all the above it is possible to conclude that for achieving higher conversions and MD selectivity with a typical NiMo/[γ-Al_2O_3 + USY] HCK catalyst one should consider diffusion limitations generated in the zeolite pore system, the number and intrinsic strength of the H/DH and acidic functions and their proximity. Mo is known to interact better with alumina than with silica [36] and consequently the hydrogenating phase supported on alumina–zeolite mixed supports will preferably be found on the alumina binder. If this is so, then the distance between the H/DH function on the Al_2O_3 and the acid sites of the zeolites is not optimized [3,37].

In this work, we will show the convenience of introducing Ni in the zeolite component of NiMoS/[γ-Al_2O_3 + USY] catalyst using a squalane HCK model reaction. In this way, a better balance between the H/HD and acidic function is achieved with the corresponding benefit on activity and selectivity to MD.

2. Experimental

2.1. Zeolites, supports and catalysts preparation

Parent zeolite used in this study was a commercial NH_4^+–USY zeolite (CBV712, Zeolyst International). Nickel was introduced onto the zeolite using incipient wetness impregnation of a nickel nitrate hexahydrate ($Ni(NO_3)_2$, $6H_2O$, Sigma–Aldrich) solution. The resultant impregnated zeolite was dried overnight at 120 °C and calcined at 450 °C during 2 h (heating rate of 5 °C/min) under dry air (2 L/h/g of zeolite). Samples will be referred as USY–Ni(*x*), where *x*, varying from 0 to 3.1, is the zeolite Ni content in wt.%. The parent zeolite will be referred as USY–P.

Supports were prepared by mixing the USY–Ni(*x*) zeolite powder with boehmite (Pural SB-3, Condea Chemie Gmbh) in the presence of a nitric acid solution and shaped to form trilobe extrudates. Extrudates were dried at 120 °C overnight and calcined at 600 °C during 2 h (heating rate of 5 °C/min) under dry air (1.5 L/h/g of support).

Catalysts were prepared by incipient wetness impregnation of the extrudates in order to load 13.0 wt.% of MoO_3, 2.7 wt.% of NiO and 3.1 wt.% of P_2O_5 on all catalysts. Then they were dried at 120 °C overnight and calcined at 500 °C during 2 h (heating rate of 5 °C/min) under dry air (1 L/h/g of catalyst). Supports and catalysts are referenced using the name of their parent zeolite followed by –S for Supports and –C for Catalysts, i.e., USY–Ni(*x*)–S or USY–Ni(*x*)–C.

2.2. Materials characterization

Metal contents of zeolites and catalysts were determined by X-ray fluorescence spectroscopy (XRF) using a Philips PW 2404. Fine powders of the materials were analyzed directly (for P content) or after they were fused with a suitable flux at 1000 °C and cast into the shape of a glass bead (for Ni, Mo, Si and Al contents). All results are expressed on the basis of the dry materials.

FT-IR spectra were recorded with a Nicolet Nexus 2 spectrometer equipped with an adsorption cell. The zeolite (ca. 20 mg) was pressed into a self supported wafer and activated under secondary vacuum in the IR cell. The sample was first pre-treated at 150 °C during 6 h and heated up to 350 °C at a rate of 2 °C/min. This temperature was maintained for 2 h before decreasing to the adsorption temperature. Pyridine was, then, contacted with the zeolites at 150 °C until saturation. The physisorbed pyridine was desorbed at 150 °C during 2 h and a spectrum was recorded. Then, desorption steps were applied at 250 °C and 350 °C during 1 h and IR spectrum were recorded after each desorption step. Quantity of Brønsted and Lewis acid sites have been obtained from the integrated peak at ca. 1550 and 1450 cm^{-1} respectively using molar extinction coefficients determined in the laboratory for Brønsted acid sites (1.04 cm/μmol) and from the literature for Lewis acid sites (2.22 cm/μmol) [38].

Nitrogen adsorption measurements were carried out with a Micromeritics ASAP 2420 at 77 K. Microporous volumes were determined by the *t*-plot method using the Harkins-Jura equation. BJH method was used to get information on pore distribution.

Mercury intrusion experiments at room temperature were applied on supports and catalysts using a Micromeritics AutoPore IV. Information on pore distribution were obtained from the Hg volume absorbed versus pore diameter plots.

Transmission electron microscopy (TEM) has been performed with a JEOL JEM 2100F apparatus. The operating voltage was 100 kV. Catalyst extrudates have been grinded and the resulting powder has been embedded in an epoxy resin. Ultra thin cuts (70 nm) have been obtained by cutting the resin with an ultramicrotome equipped with a diamond knife, and, thin cuts were deposited on a carbon-coated copper grid.

The X-ray diffraction (XRD) powder patterns were recorded with a PANalytical X'Pert PRO MPD θ–θ diffractometer using CuKα radiation. The unit cell size of the zeolites was determined using a full pattern matching procedure with the TOPAS software and the sample crystallinity index was determined using the D3906 ASTM method.

2.3. Catalytic tests

Catalytic activity measurements for toluene hydrogenation (*HYD*) and squalane HCK were carried out in a continuous fixed-bed down-flow reactor at a total pressure of 6 MPa. First, the catalyst (20 cm^3) was sulfided in situ at 350 °C with a feed containing cyclohexane (73.6 wt.%), toluene (20 wt.%), Di-Methyl-Di-Sulfide (5.9 wt.%) and aniline (0.5 wt.%) under the operating conditions given in Table 1. Then, the toluene hydrogenation test was performed using the same feed but with different operating conditions as shown in Table 1. Liquid products were analyzed by gas chromatography (GC) equipped with a PONA column and a Flame